Available online at www.sciencedirect.com
ScienceDirect
Polymer 48 (2007) 7623–7631
polymer
www.elsevier.com/locate/polymer

Characterization of water in bacterial cellulose using dielectric spectroscopy and electron microscopy

Kristina Gelin [a], Aase Bodin [b], Paul Gatenholm [b], Albert Mihranyan [c], Katarina Edwards [a], Maria Strømme [c,*]

[a] *Department of Physical and Analytical Chemistry, Uppsala University, P.O. Box 579, SE-751 23 Uppsala, Sweden*
[b] *Biopolymer Technology, Department of Chemical and Biological Engineering, Chalmers University of Technology, Kemivägen 10, SE-412 96 Göteborg, Sweden*
[c] *Division of Nanotechnology and Functional Materials, Department of Engineering Sciences, The Ångström Laboratory, Uppsala University, Box 534, SE-751 21 Uppsala, Sweden*

Received 23 August 2007; received in revised form 24 October 2007; accepted 26 October 2007
Available online 1 November 2007

Abstract

It is shown that only 10% of the 99 wt% water present in bacterial cellulose (BC) gels, produced by *Acetobacter xylinum*, behave like free bulk water; the majority of the water molecules in the gels is more or less tightly bound to the cellulose. The magnitude of the diffusion coefficients of ions transported in the water phase of the BC gels as well as the information contained in freeze fracture transmission electron microscopic images of the gel structures indicates that the bulk-like water is confined in ''lakes'' rather than forming a continuous phase throughout the gel. Water desorption isotherms suggest that these ''lakes'' decrease in size with increasing oxygen concentration used during the biosynthesis process of the gels.

Keywords: Dielectric spectroscopy; Bacterial cellulose; Water

1. Introduction

Since the extraordinary structure of bacterial cellulose (BC) was described more than a century ago [1,2], the material has been extensively analyzed and characterized [3–7]. The ultrafine structure of BC microfibrils, which bear certain resemblance to collagen networks, makes this material interesting for various biomaterial applications. Some applications have been suggested, including as artificial blood vessels [8], as scaffolds for treatment of burn ulcers [9], and in tissue engineering of cartilage [10].

The supramolecular structure of BC is markedly different from other native cellulose types despite the identical chemical composition. The native cellulose derived from *Acetobacter xylinum* bacteria is rich in 1α-cellulose (algal/bacterial type) whereas that from land plants is rich in 1β-cellulose (cotton-ramie type). The width of the cellulose crystallite of land plant cellulose is about 4 nm while that from algal/bacterial sources is about 30 nm. The difference between the cellulose types can be traced back to the differences in the cellulose synthase complexes which determine the size and thickness of the cellulose microfibrils. The cellulose synthase complexes in land plants are arranged as solitary rosettes consisting of six hexagonal subunits producing thin microfibrils, whereas the cellulose synthase complexes in more primitive organisms, e.g. algae, are arranged into large rectangular units rather than rosettes.

Unlike native cellulose obtained from other sources, i.e., land plants or algae, BC does not contain collateral biogenic compounds like lignin, pectin and hemicellulose requiring purification and can therefore be separated in its purest form during the extracellular synthesis process. The cellulose derived

* Corresponding author. Tel.: +46 18 4717231.
E-mail address: maria.stromme@angstrom.uu.se (M. Strømme).

0032-3861/$ - see front matter © 2007 Elsevier Ltd. All rights reserved.
doi:10.1016/j.polymer.2007.10.039

this way has a remarkable ability to retain large amounts of water rendering this material unique attributes: in addition to the similarity between the BC microfibril networks and collagen it is most likely the high water content that renders its biocompatible properties [11,12] important for *in vivo* applications. A detailed study of the supramolecular structure of native BC, normally containing approximately 99 wt% of water, showed that no water is incorporated in the crystalline microfibrils of this material, instead the microfibrillar units are surrounded by a hydration shell and a small number of non-crystalline tie molecules most likely connect the crystalline microfibrils laterally [13]. Also for moist cellulose structures of land plant or algal origin, water is situated *outside* the crystalline microfibrils [14,15] although usually in a much lower amount.

The rheological properties of reticulated bacterial cellulose in terms of gel strength have previously been described [16,17] and they are in many aspects similar to those of algal cellulose based gels [18]. However, there are hitherto no reports wherein water–cellulose interactions in BC have been analyzed in detail.

The purpose of the present study is to perform a detailed analysis of the water interaction properties in as-biosynthesised BC gels using dielectric spectroscopy, a method that previously has been proven useful for extracting information about water transport processes and interactions within a number of biopolymers [19] including celluloses of various origins [20–22]. The dielectric spectroscopic results are discussed and compared to gels originating from the green algae *Cladophora* and moist powder of microcrystalline land plant derived cellulose.

Freeze fracture Transmission Electron Microscopic (TEM) images and cryogenic TEM pictures of BC microfibrils are also for the first time presented, as well as Environmental Scanning Electron Microscopic (ESEM) images and water desorption isotherms of never-dried and non-frozen BC gels.

2. Experimental

2.1. Materials

2.1.1. Bacterial cellulose gels

The production of different BC gels at different oxygen concentrations (20, 35, 50 and 100%) was carried out as previously described [23]. A complex medium (CSL) was used as fermentation medium [24]. The strain used for the biosynthesis was *A. xylinum* subsp. *sucrofermentas* BPR2001, trade number 1700178™. The strain was purchased from the American Type Culture Collection. Six cellulose-forming colonies were cultivated for 2 days in Rough flasks yielding a cell concentration of 3.7×10^6 cfu/ml. Bacteria were liberated from the resulting BC hydrogel by vigorous shaking and 2.5 ml was added to each fermentation vessel and cultivated onto a gas permeable mould, i.e., a poly(dimethylsiloxane), PDMS, tube. The morphology of the biopolymer network becomes a replica of the PDMS template and can be extracted from the mould as a cellulose tube. The BC tubes and the hydrogel from the preculture were purified by boiling in 0.1 M NaOH at 60 °C for 4 h and thereafter repeated boiling in Millipore™ water. The BC tubes were steam sterilized by autoclaving for 20 min (120 °C, 1 bar) and stored in a refrigerator until characterization. The tubular gels were cut longitudinal to enable dielectric spectroscopic measurements through the tube wall. BC gel from the preculture, produced at 20% of oxygen, was disintegrated with a blender before characterization with freeze fracture TEM and cryo TEM.

2.1.2. Cladophora cellulose gels

Cladophora cellulose (CC) powder was produced as previously described [14]. Briefly, the algal cellulose was extracted from *Cladophora* sp. algae harvested from the Baltic Sea. α-Cellulose was extracted by treating the algae with $NaClO_2$ in an acetic buffer, followed by washing in NaOH. The extracted material was depolymerised by acidic hydrolysis and grinding and then, as a suspension, spray-dried to form cellulose powder. The cellulose powder samples were sieved prior to preparation of the gels, and the fraction between 45 and 106 μm was separated. The CC gels, containing 2 wt% CC and 98 wt% water were prepared as described in Ref. [18], by employing a sonication technique that first dispersed the individual cellulose particles in small volumes of liquid. This procedure produces powerful shearing action and causes the cellulose agglomerates in the liquid to become intensely agitated and eventually disrupted into fine individual particles, i.e., crystallites or small crystallite aggregates.

2.2. Methods

2.2.1. Dielectric spectroscopy

In dielectric spectroscopy, a sinusoidal voltage is applied across a sample localized between two electrodes in a probe station and the frequency of the voltage is scanned from a maximum to a minimum value. The measured current response due to charged species present in the sample can be interpreted in terms of several interrelated complex frequency-dependent parameters such as impedance, conductance, capacitance and dielectric permittivity. For example, the complex permittivity ε of a sample is obtained from the measured complex capacitance C as

$$\varepsilon = \varepsilon' - \mathrm{i}\varepsilon'' = \frac{C}{C_0}, \tag{1}$$

where C_0 is the capacitance of the empty measuring cell, and ε' and ε'' are the real and imaginary parts of the permittivity, respectively. For the measuring cell used in the present work $C_0 = \varepsilon_0 A/d$, where A and d are the electrode area and electrode separation distance, respectively, and ε_0 is the permittivity of free space (8.854×10^{-14} F/cm).

In this work an analysis method described earlier [25] is employed and specifically focuses on the real part, σ', of the complex conductivity, σ, which is related to the real part, G', of the measured conductance and to the imaginary part, ε'', of the dielectric permittivity as

$$\sigma' = \frac{d}{A}G' = \omega\varepsilon_0\varepsilon''. \quad (2)$$

Here ω is the angular frequency.

At high frequencies, the movable ions in a sample will only have time to travel a very short distance before the sign of the applied sinusoidal field is changed and the ions are forced to change their direction of motion. Thus, at high enough frequencies, the ions will be able to move unhindered by the electrodes as if they were free. The conductivity associated with this dc-like, unrestricted, motion can be expressed as

$$\sigma_{dc} = \frac{nq^2D}{kT}, \quad (3)$$

where n is the concentration of carrier ions, q is the ionic charge, D is the ion diffusion coefficient, and kT is the thermal energy.

At lower frequencies the movement of ions is hindered by the electrodes – a phenomenon referred to as electrode polarization – and under certain circumstances, such that the electric fields created by charge separation near the electrode surfaces do not induce non-linear effects [27,28], the charge carrier concentration can be extracted from the permittivity spectrum using the following relation [29]:

$$n = \left(\frac{\sigma_{dc}}{\sqrt{(X-1)}\varepsilon_0\varepsilon_s'\omega_X}\right)^4 \frac{\varepsilon_0\varepsilon_s' kT}{q^2d^2}. \quad (4)$$

Here ε_s' is the real part of the dielectric permittivity in the high-frequency region where σ' is dominated by dc-like ion conduction and ω_X is the angular frequency for which $\varepsilon'(\omega_X) = X\varepsilon_s'$.

The dielectric spectroscopic measurements were carried out with a Novocontrol Alpha-AN dielectric measurement system (Novocontrol Technologies GmbH & Co. KG). The samples were placed between two gold-plated brass electrodes having a diameter of 10 mm and the electrode separation was set by a micrometer screw, Fig. 1. A guard ring was incorporated around the signal electrode to reduce stray capacitance and edge effects and the entire electrode arrangement was enclosed in a sealed stainless steel container to provide an electrically shielded environment. A 100% relative humidity (RH) environment inside the container was ensured when water was placed in the bottom of the stainless steel container. The temperature was controlled with an incubator (Incucell IC 55, BMT a.s., Brno, Czechnia) for temperatures above room temperature (RT) and a thermometer with an accuracy of ±0.2 °C was located inside the container. Dielectric spectra in a frequency range of 10^{-2}–10^6 Hz were recorded for five temperatures in the interval between RT and 55 °C. Each temperature scan was finalized by recording a RT spectrum to investigate if irreversible changes in the structure were introduced by raising the temperature. The measurements were carried out for at least four samples of each BC type investigated.

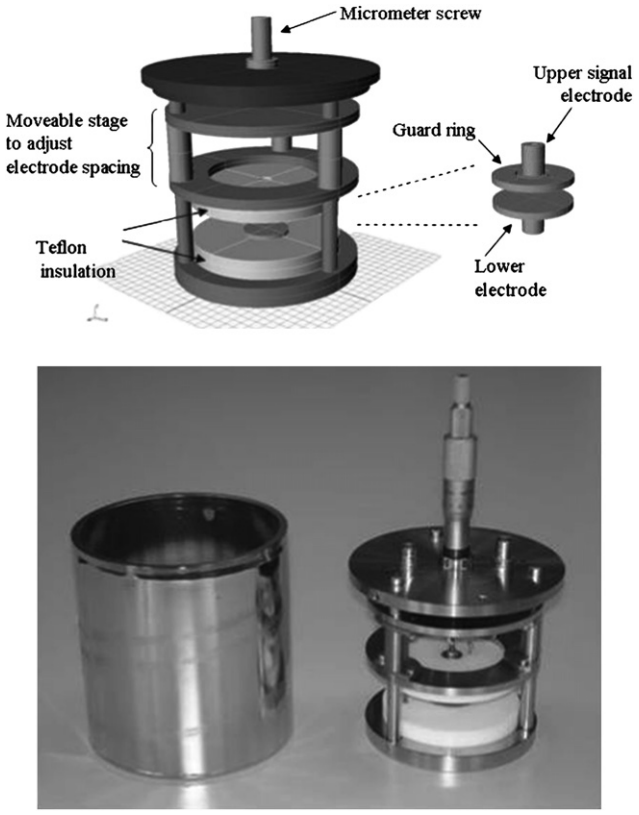

Fig. 1. Dielectric measurement cell described in detail in Ref. [26].

2.2.2. Water desorption isotherms

The equilibrium moisture content was obtained from gravimetrical measurements using a AX504DR balance (Mettler Toledo) after the samples had been stored in desiccators for 6 days at RT over saturated salt solutions of NaCl, $Mg(NO_3)_2$, K_2CO_3, NaI, LiI, and $CaCl_2$ corresponding to 75, 54, 43, 39, 19, and 0% RH, respectively. Prior to the measurements, the samples were stored at RT at 100% RH, over a water bath for 24 h. The mass of water present in the samples per mass of dry cellulose was calculated, based on the assumption that the powders stored over the $CaCl_2$ salt solution was completely dry, as

$$\text{g water/g dry cellulose} = \frac{m_{\text{after } X\%\text{ RH}} - m_{\text{cellulose } X\%\text{ RH}}}{m_{\text{cellulose } X\%\text{ RH}}}, \quad (5)$$

where $m_{\text{after } X\%\text{ RH}}$ denotes the actual sample mass measured after the sample has been stored at X% RH and $m_{\text{cellulose } X\%\text{ RH}}$ denotes the dry cellulose part of this mass. Whereas $m_{\text{after } X\%\text{ RH}}$ is measured directly, $m_{\text{cellulose } X\%\text{ RH}}$ can be calculated according to the following equation:

$$m_{\text{cellulose } X\%\text{ RH}} = \frac{m_{\text{after } 0\%\text{ RH}} \times m_{\text{before } X\%\text{ RH}}}{m_{\text{before } 0\%\text{ RH}}}. \quad (6)$$

Here $m_{\text{before } X\%\text{ RH}}$ is the measured mass of the sample before it is placed in the X% RH desiccator, $m_{\text{after } 0\%\text{ RH}}$ is the measured mass of the sample that has been stored at 0% RH in the $CaCl_2$ desiccator and $m_{\text{before } 0\%\text{ RH}}$ is the measured mass of

that particular same sample before it was placed in the $CaCl_2$ desiccator.

2.2.3. Environmental scanning electron microscopy

An environmental scanning microscope of type Philips XL 30 ESEM-FEG with standard Peltier heating and cooling stage was employed for microscopic observations of BC and CC gel samples. The RH in the measuring chamber was kept at 77% by setting the chamber pressure to 4 Torr through a computer-stabilized needle valve and the sample temperature was maintained at +5 °C by means of a Peltier stage.

2.2.4. Cryogenic transmission electron microscopy

Cryogenic TEM (cryo TEM) images of disintegrated BC20 samples were obtained by using a Zeiss EM 920 A transmission electron microscope (Carl Zeiss Inc., Oberkochen, Germany). The technique is described elsewhere [30,31]. The samples were prepared at 25 °C. Images were taken in zero-loss bright field mode with an acceleration voltage of 80 kV.

2.2.5. Freeze fracture transmission electron microscopy

The freeze fracture replica technique was conducted on disintegrated BC20 samples diluted 30 times in water. A copper grid (300 mesh) was dipped in the BC solution and placed between two copper specimen carriers and thereafter quick-frozen in liquid propane at −180 °C in a BAL-TEC JFD 030 Jet Freeze Device (BAL-TEC AG, Liechtenstein). The frozen samples were transferred to a BAL-TEC BAF 060 freeze fracture system (BAL-TEC AG, Liechtenstein) where the samples were fractured at −150 °C. The fractured surfaces thereafter were immediately replicated by evaporation of a 3 nm platinum–carbon coating followed by a 20 nm carbon coating. The films were deposited from two electron guns positioned at 45° and 90° (relative to the fractured sample surfaces), respectively. The replicas were floated off in distilled water and the replica pieces were then cleaned in 70% sulfuric acid for 30 min followed by distilled water for 5 min, 14% sulfuric acid for 30 min and finally two times for 5 min in distilled water.

The clean replicas were collected on a copper grid and studied with a Zeiss LIBRA® 120 transmission electron microscope (Carl Zeiss NTS GmbH, Oberkochen, Germany). Images were taken in zero-loss bright field mode with an acceleration voltage of 120 kV.

3. Results and discussions

3.1. Dielectric spectroscopy

Fig. 2 shows the real part of the permittivity recorded at RT for the four types of BC gels and the one type of CC gel under study. For comparison ε' for one of the most commonly used microcrystalline cellulose (MCC) powder types used in pharmaceutical applications, Avicel pH 101, equilibrated at 22% RH [32] as well as ε' for deionized water [25] is also included in the figure. By comparing the BC gel spectra to that of the moist MCC powder, one finds that the high-frequency values

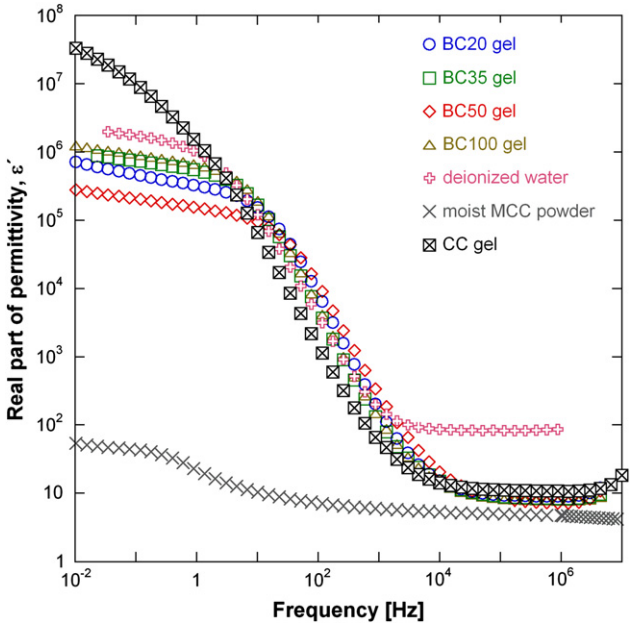

Fig. 2. Real part of the permittivity for bacterial cellulose (BC) gels produced at different oxygen concentrations, for a *Cladophora* cellulose (CC) gel, for MCC powder equilibrated at 22% RH from Ref. [32], and for deionized water from Ref. [25]. All spectra were recorded at room temperature.

of ε' for the BC gels are in the range 7.3–8.7 and substantially higher than that for the moist MCC powder. In an earlier study of the effect of water on dielectric spectra of MCC powders it was found that increasing the amount of water from 0 to 6 wt% in the MCC powder bed did not increase the magnitude of the high-frequency ε', indicating that water was bounded in the cellulose structure in such a way that it did not contribute to the dipolar dielectric response [22]. As the high-frequency ε' for dry cellulose is ∼4.5 and the corresponding value for free water is ∼80, water clearly has a significant effect on the high-frequency dielectric response of the BC gels under study. Considering that there is ∼99 wt% water present in the gels [13], however, a simple calculation shows that only 10% of the water present behaves like free bulk water; the majority of the water molecules in the BC gel structures is rather tightly bound to the cellulose structure. For the CC gel under study the high-frequency ε' is ∼11, indicating that the ability to bind water strongly in this structure is slightly lower than that in the BC gels. Significant differences in ε' amongst the BC gels produced at different oxygen concentrations could not be revealed. The variation in frequency for which ε', due to electrode polarization, rises from its high-frequency plateau value to its low frequency constant value for the specific measurements displayed in Fig. 2, is a function of gel thickness only; the thinner the gel (in Fig. 2 BC50 is the thinnest), the higher the electrode polarization onset frequency [28].

Fig. 3 shows σ' for the BC and CC gels under study together with the same parameter for deionized water. The corresponding parameter for MCC powder equilibrated at 22% RH – and thus containing ∼3 wt% water [33] – is several orders of magnitude lower [32]. From the figure it is apparent

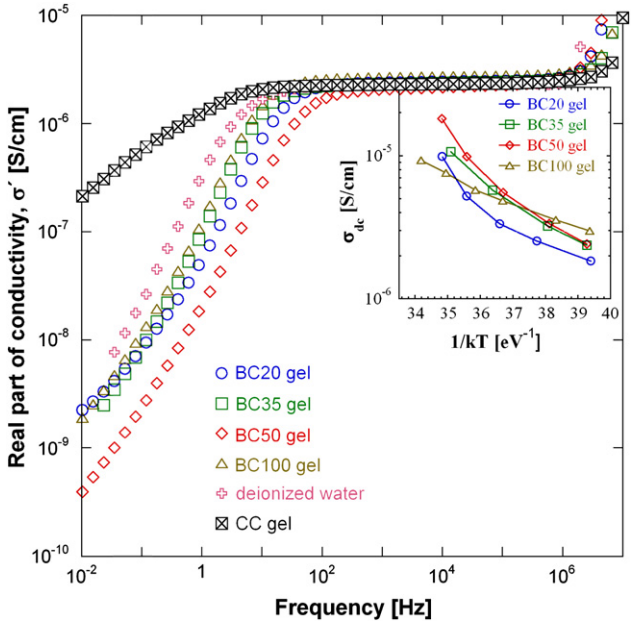

Fig. 3. Real part of conductivity for bacterial cellulose (BC) gels produced at different oxygen concentrations, for a *Cladophora* cellulose (CC) gel and for deionized water from Ref. [25]. The inset shows the parameter σ_{dc} extracted from single measurements on the four types of BC gels under study performed at five different temperatures.

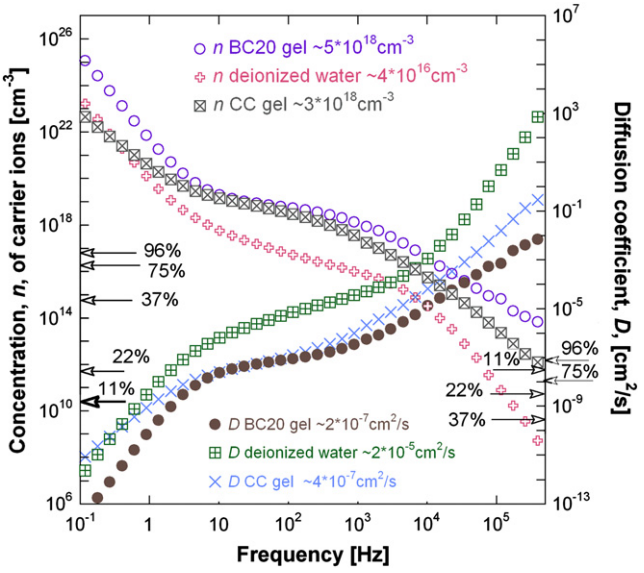

Fig. 4. Diffusion coefficients, D, and charge carrier concentrations, n, as obtained from Eqs. (3) and (4), respectively, for a recording on a BC20 gel and a CC gel sample together with the same quantities for deionized water from Ref. [25]. Included in the figure are the D and n values obtained for MCC powders equilibrated at the indicated RHs from Ref. [33] and thus containing various amounts of water. The approximately constant n and D regions around 10^2 Hz for both the gels and the deionized water signify the region of validity for Eq. (4).

that the unhindered ionic conductivity in the BC and CC gels, σ_{dc} described by Eq. (3), is of the same order of magnitude as for deionized water. From the shape of the σ' vs. frequency curves it is also clear that the number of charge carriers as well as the diffusion coefficient of the ionic species governing the conduction can be extracted using Eqs. (3) and (4) [25]. Again, the reason for the different onset frequencies of electrode polarization (decreasing σ' towards lower frequencies) lies in the different electrode separations used in the individual measurements. While for the BC gels the electrode separations were between 20 and 80 μm, the separations in the deionized water experiment [25] and the CC gel experiment displayed in the figure were 25 and 240 μm, respectively.

Included in Fig. 3 is an inset showing σ_{dc} extracted from single measurements on the four types of BC gels under study performed at five different temperatures. From the temperature scans it was found that the temperature could be raised only to ~45 °C without introducing irreversible changes in the gel structure. After recordings performed at higher temperatures, the initially recorded RT spectra could not be retained. This is in accordance with earlier findings [34] showing that at a temperature of ~320 K (or 47 °C) chemical and/or structural changes related to water sorption–desorption in the BC set in. Thus, to extract the activation energies of the charge transport processes in the BC gels only the Arrhenius behaving data points below ~45 °C are used. These data are presented and discussed below.

Fig. 4 shows D and n as obtained from Eqs. (3) and (4), respectively, for a recording on a BC20 gel and a CC gel sample together with the same quantities for deionized water from Ref. [25]. Included in the figure are the diffusion coefficient and the concentration of ionic charge carriers in MCC powder from Ref. [33] equilibrated at the indicated RHs and thus containing various amounts of water. The approximately constant n region around 10^2 Hz for both the gels and the deionized water signifies the region of validity for Eq. (4). At lower frequencies, the linearity assumption for the internally generated electric fields no longer holds and an incorrect rise in n towards lower frequencies results. From the approximately constant n region, the charge carrier concentration displayed in the figure could be extracted. Similarly, the D values extracted from the plateau region between 10^2 and 10^3 Hz are also displayed. By comparing all displayed values it is clear that the concentration of charge carriers contributing to the conductivity in the liquid phase of the BC and CC gels is significantly larger than those in an MCC powder structure and also than in deionized water. The fact that n is larger than that in deionized water clearly shows that there are other ionic species present in the gels than the water constituent ions (H_3O^+ and OH^-). These ions are most likely Na^+ ions or other smaller ions remaining from the purification of CC and BC. Whereas the average diffusion coefficient for water constituent ions in deionized water is $\sim 2 \times 10^{-5}$ cm^2/s, D in the BC20 and the CC gels are of the same order of magnitude as in a moist MCC sample (almost always containing Na^+ ions in addition to H_3O^+ and OH^-), viz. $\sim 10^{-7}$ cm^2/s. This indicates that the long range ionic charge transport mechanism in both the BC and the CC gels with water contents of around 99 and 98 wt%, respectively, is similar to that in MCC containing only a few wt% of water. The presence of a continuous bulk liquid phase in the gels would constitute an easy

conduction path for water constituent ions as well as other small ions and would lead to diffusion coefficients of the same order of magnitude as those for ions in free water. From the low diffusion coefficients found here, the conclusion can be drawn that ~10% of free water present in the gels – as extracted from the high-frequency dielectric response – does not form a continuous phase throughout the gels, but rather is confined in isolated "lakes" in the microfibril network. This is also in agreement with percolation theory, since percolation of a component in a three-dimensional network seldom occurs at volume ratios below 20% [35].

Water vapour adsorption on MCC powder of land plant origin has been shown to occur in different steps, and three various binding strengths (tightly bound, less tightly bound and bulk water) of the water molecules to the cellulose structure have been identified [36]. In the first step, each water molecule attaches to two carbon-6 hydroxyl (6-OH) groups on neighbouring cellulose chains. A moisture content of ~1.5 wt% in MCC represents a ratio of one water molecule to two monomer units in the cellulose. The water adsorbed in this step is tightly bound [37]. At moisture contents exceeding ~1.5 wt%, it is still energetically favourable for the water molecules to bind to the 6-OH groups. Hence, during the adsorption process above ~1.5 wt% moisture content, the tightly bound water molecules present in the structure have to let go of one of the hydrogen bonds to leave room for the incoming water molecules to attach to a 6-OH group. At ~3 wt% moisture, each water molecule is attached to the cellulose chain by only one hydrogen bond and is thus less tightly bound than that in the initial step. On adding further moisture to the MCC structure, polymer–polymer hydrogen bonds in the cellulose may be broken to make more primary binding sites available. Water may also attach to the water molecules already bound to the cellulose by dipole attraction or by weak hydrogen bonds [37]. At humidities higher than ~60% RH (~6 wt% moisture) water can also bind to other water molecules, including those not bound to primary sites [36] and, thus, form a more weakly bound bulk liquid phase. Considering that only ~10% of the 99 wt% water present in the BC gels is likely to be present in a free bulk liquid phase, the three-binding-strength model proposed for water adsorption to MCC powder cannot be used to describe the energetic of the water binding mechanism during the BC gel biosynthesis process. Both CC powders [14] and never-dried [38] and freeze-dried [39] BC gels have surface areas exceeding that of MCC powder [14] by approximately two orders of magnitude, and thus have considerably more primary water binding sites available: the fact that much less CC powder was needed to form solid–gel mixtures as compared to MCC powder has previously been explained by the large surface area available for water to bind to CC [18].

Fig. 5 shows the activation energies of the conduction process extracted from curves of the type shown in the inset of Fig. 3 at temperatures between RT and ~45 °C as well as the RT diffusion coefficients related to this process for the BC gels under study. A variation in the diffusion coefficient with varying oxygen concentration at which the BC gels were biosynthesised may be noticed. The diffusion coefficient decreases slightly with increasing oxygen concentration for oxygen concentrations below 50%, while the value of D for BC100 gels is similar to that for BC20 gels. The activation energy follows an, not statistically confirmed, opposite trend with the lowest value for the BC100 gels. To our knowledge there are no literature data available on the activation energy for the diffusion process in moist land plant derived MCC in the temperature interval slightly above RT. Earlier studies performed at higher temperatures on dried BC containing only small amounts of moisture have shown on diffusion activation energies above 1.2 eV (118 kJ/mol). The values presented in Fig. 5 are considerably lower and only slightly higher than 0.1 eV, which is the activation energy of diffusion of protons in free bulk water [40].

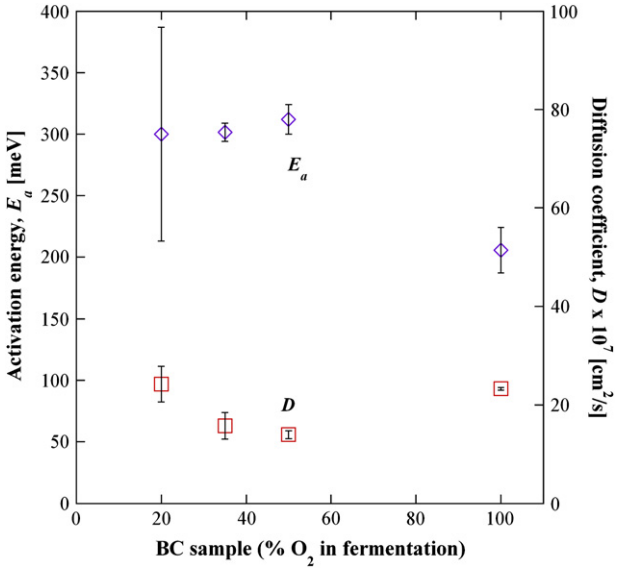

Fig. 5. Activation energies of the conduction process extracted from curves of the type shown in the inset of Fig. 3 at temperatures between RT and ~45 °C as well as the RT diffusion coefficients related to this process for the BC gels under study. The error bars indicate absolute variations over three measurements.

3.2. Desorption isotherms

Fig. 6 shows the water desorption isotherms of the BC gels under study. Incorporated as an inset in Fig. 6 are earlier presented [14] desorption isotherms recorded on powders of MCC (Avicel pH 102) and on CC. In the high-humidity region the onset of desorption in the BC gels is clearly shifted towards lower RHs with increasing oxygen concentrations during the fermentation process. According to the Kelvin equation [41] this shift could be indicative of a decrease in size of the capillaries – the above-mentioned "lakes" hosting bulk water – with increasing oxygen concentration. This conclusion is in accordance with previously reported data [15] showing that the diameter of the largest capillaries in *Cladophora* cellulose powder is significantly smaller than the corresponding one for MCC powder, and as can be seen in the inset the major

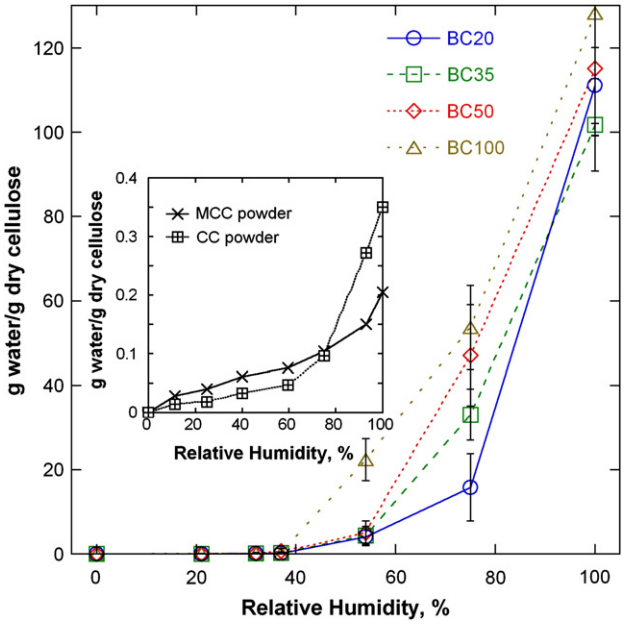

Fig. 6. Water desorption isotherms of the BC gels under study. The inset shows the corresponding isotherms recorded on powders of MCC and *Cladophora* cellulose from Ref. [14].

desorption in the CC powder takes place at a lower RH than in MCC. By further comparison between the cellulose powder isotherms and the BC gel isotherms it is found that the BC gels need to be dried at RHs as low as 20–30% to reach the same low level of moisture content as the powders.

3.3. Electron microscopy

Cryo TEM images of disintegrated BC can be viewed from Fig. 7. Individual fibres of about 30 nm in width can be clearly distinguished. These fibres are most likely the individual crystalline microfibrils as several previous SEM examinations have shown that the microfibrils in *A. xylinum* produced cellulose have this size. The figure panel to the left shows approximately 5–10 microfibrils assembled in a twisted ribbon. The width of the ribbon is approximately 200 and 400 nm at the narrowest and widest parts, respectively.

Fig. 8 shows ESEM images recorded at 77% RH of the inner side of the BC gel tubes. At this RH the gels contain between 10 and 40 wt% water, Fig. 6. An earlier study has revealed that more cellulose is produced at higher oxygen concentrations [23]. Upon water desorption, the BC gel tubes become pleated, which results in structures of 10–20 μm in size. The creases seem to be getting denser at higher oxygen concentration probably due to higher amount of cellulose in these BC gel tubes. At short length scales the network of microfibril bundles also seen in the cryo TEM images are clearly visible.

Two freeze fracture micrographs of the BC are shown in Fig. 9. The BC is known to be composed of flat-shaped microfibrils, each consisting of several thousands of glucan chains [5], and in both panels presented this flat-shaped structure can be distinguished. More interesting, however, is that these pictures allow for a detailed visual examination of the arrangement of microfibrils in ribbons and also give some support to the above set-forth "lake" assumption. The microfibrils are clearly woven together in a network that leaves some open space in which it is likely that water may exist in bulk phase. A detailed analysis of the size of these lakes should, however, not be carried out with the presented freeze fracture images as base since the BC was diluted prior to examination.

4. Summary and concluding remarks

Dielectric spectroscopy was employed to characterize the structural properties of water and the associated charge transport mechanisms in cellulose gels produced by *A. xylinum* bacteria at various oxygen concentrations. The frequency-dependent dielectric behaviour of the gels was compared to that for gels of cellulose extracted from the green algae *Cladophora* as well as to moist powders of microcrystalline land plant derived cellulose. Water desorption isotherms, ESEM, freeze fracture TEM and cryo TEM were also employed to obtain information about the BC nanostructure.

Small variations in the diffusion coefficient of water constituent ions and ions remaining from the gel purification process transported in the water phase of the BC gels were found between gels biosynthesised at different oxygen concentrations; the lowest diffusion coefficient was found for gels produced at an oxygen concentration of 50%.

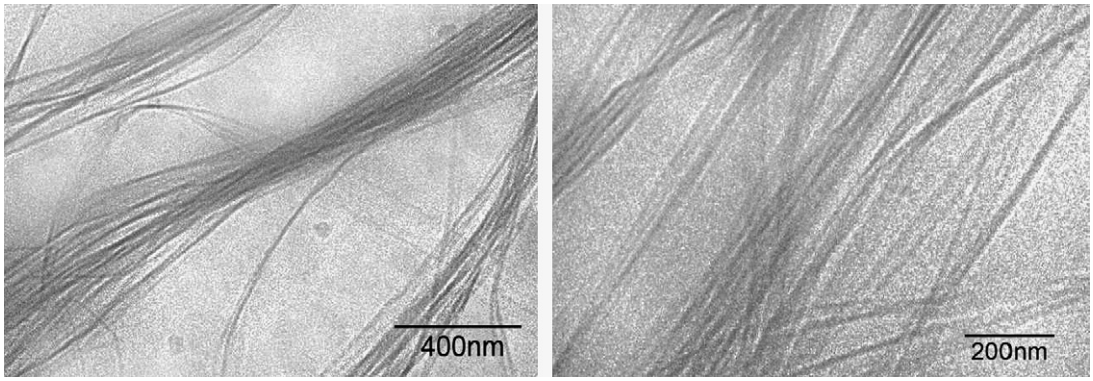

Fig. 7. Cryo TEM images of disintegrated BC20.

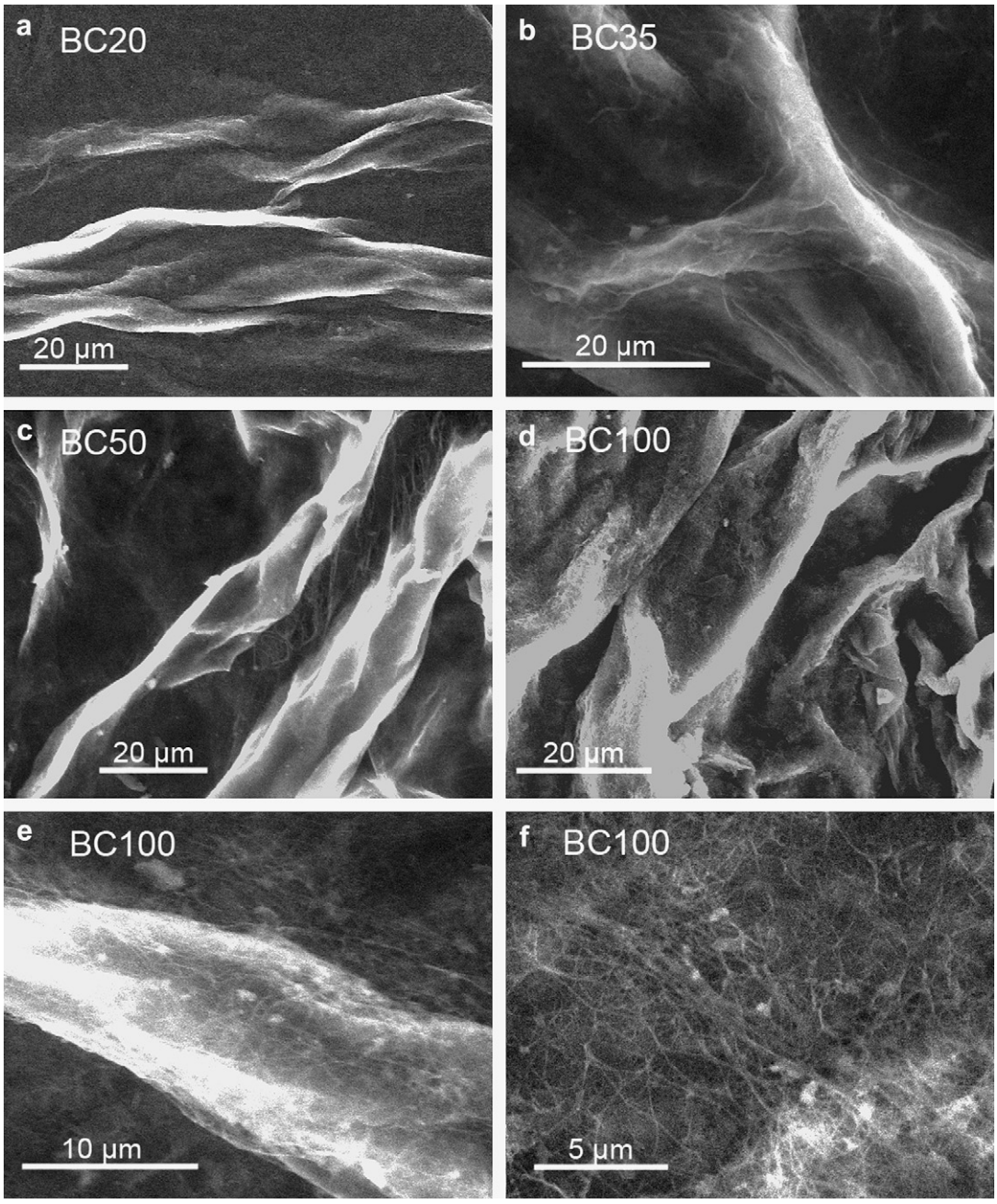

Fig. 8. ESEM images recorded at 77% RH on the inner side of the BC gel tubes. At this RH the gels contain between 10 and 40 wt% water.

Upon water desorption, the BC gel tubes became pleated, resulting in structures of 10–20 μm in size as observed in the ESEM. A densification of pleats with increasing biosynthetic oxygen concentration was noted and explained by an increasing amount of cellulose.

It was found that only about 10% of the 99 wt% water present in the BC gels behaved like free bulk water; the majority of the water molecules in the gels was more or less tightly bound to the cellulose. This number was similar, but slightly lower than the corresponding one for CC gels indicating that the ability to bind water strongly in never-dried BC gels is slightly higher than that in the CC gel structure. This indicates that never-dried or as-biosynthesised BC gels have better ability than CC to strongly bind water.

The magnitude of diffusion coefficients extracted from dielectric spectroscopic measurements as well as the information contained in freeze fracture TEM images indicates that the free or bulk-like water present in the BC gels is confined in ''lakes'' rather than forming a continuous phase throughout the gel structure. Water desorption isotherms suggest that these ''lakes'', hosting bulk water, decrease in size with increasing oxygen concentration used under the biosynthesis process. In the future it would be interesting to study the correspondence between the biocompatibility of BC gels and the size of the lakes discovered in the present work since the amount and state of water are assumed to be of importance for interactions with proteins and other biomolecules.

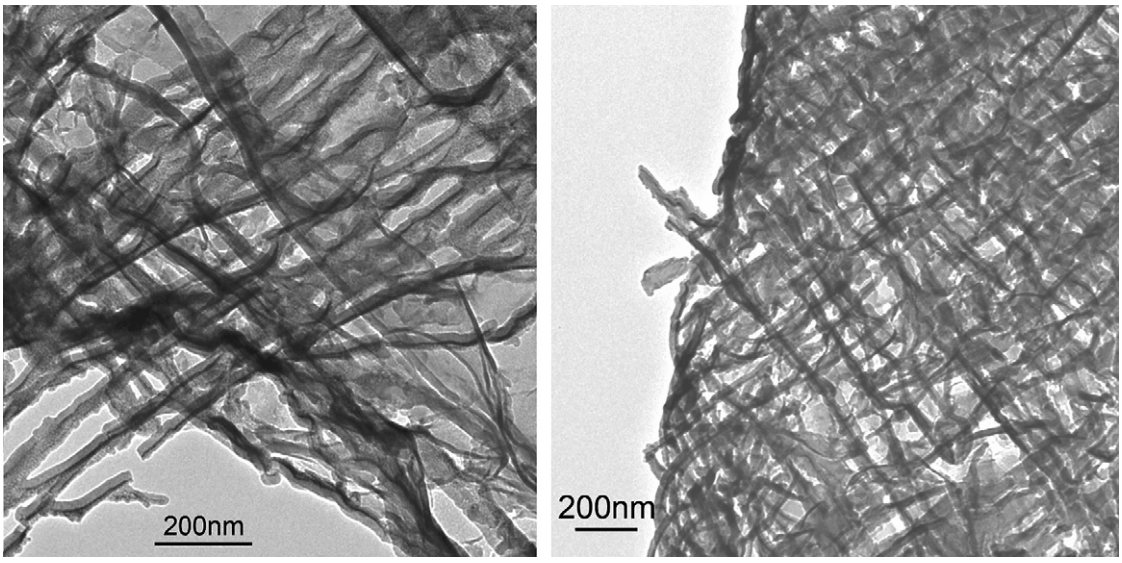

Fig. 9. Freeze fracture TEM images of disintegrated BC20.

Acknowledgements

This project was funded by The Knut and Alice Wallenberg Foundation, The Göran Gustafsson Foundation, The Swedish Research Council and The Swedish Foundation for Strategic Research. Emma Johansson is acknowledged for her help with carrying out the cryo TEM characterizations and Göran Karlsson for his help with the TEM imaging of the freeze fractured samples. One of the authors (MS) is a Swedish Royal Academy of Sciences Research Fellow and would like to thank the Academy (KVA) for their support.

References

[1] Brown AJ. J Chem Soc 1886;49:172–86.
[2] Brown AJ. J Chem Soc 1886;49:432–9.
[3] Iguchi M, Yamanaka S, Budhiono A. J Mater Sci 2000;35:261–70.
[4] Yamanaka S, Watanabe K, Kitamura N, Iguchi M, Mitsuhashi S, Nishi Y, et al. J Mater Sci 1989;24:3141–5.
[5] Brown Jr RM, Willison JHM, Richardson CL. Proc Natl Acad Sci USA 1976;73:4565–9.
[6] Cousins SK, Brown Jr RM. Polymer 1997;38:897–902.
[7] Haigler CH, Brown Jr RM, Benziman M. Science 1980;210:903–6.
[8] Klemm D, Scumann D, Udhardt U, Marsch S. Prog Polym Sci 2001;26:1561–603.
[9] Fontana JD, de Souza AM, Fontana CK, Torriani IL, Moreschi JC, Gallotti BJ. Appl Biochem Biotechnol 1990;24–25:253–64.
[10] Svensson A, Nicklasson E, Harrah T, Panilaitis B, Kaplan DL, Brittberg M, et al. Biomaterials 2005;26:419–31.
[11] Backdahl H, Helenius G, Bodin A, Nannmark U, Johansson R, Risberg B, et al. Biomaterials 2006;27:2141–9.
[12] Helenius G, Backdahl H, Bodin A, Nannmark U, Gatenholm P, Risberg B. J Biomed Mater Res A 2006;76:431–8.
[13] Fink H-P, Purz HJ, Bohn A, Kunze J. Macromol Symp 1997;120: 207–17.
[14] Mihranyan A, Piñas Llagostera A, Karmhag R, Strømme M, Ek R. Int J Pharm 2004;269:433–42.
[15] Strømme M, Mihranyan A, Ek R, Niklasson G. J Phys Chem B 2003; 107:14378–82.
[16] Watanabe K, Tabuchi M, Morinaga Y, Yoshinaga F. Cellulose 1998;5: 187–200.
[17] Shanahan CM, Zdanis DA, Clark R, Evans JM, Comfort SF. Food products containing bacterial cellulose, Publication No. WO/1997/048402; 1997.
[18] Mihranyan A, Edsman K, Strømme M. Food Hydrocolloids 2006;21: 267–72.
[19] Pissis P. In: Kupfer K, editor. Electromagnetic aquametry: electromagnetic wave interaction with water and moist substances. Berlin, Heidelberg: Springer; 2005. p. 39.
[20] Einfeldt J, Kwasniewski A. Cellulose 2002;9:225–38.
[21] Einfeldt J, Meißner D, Kwasniewski A. Cellulose 2004;11:137–50.
[22] Ek R, Hill RM, Newton JM. J Mater Sci 1997;32:4807–14.
[23] Bodin A, Bäckdal H, Fink H, Gustafsson L, Risberg B, Gatenholm P. Biotechnol Bioeng 2007;97:425–34.
[24] Matsuoka M, Tsuchida T, Matsushita K, Adachi O, Yoshinaga F. Biosci Biotechnol Biochem 1996;60:575–9.
[25] Jönsson M, Welch K, Hamp S, Strømme M. J Phys Chem B 2006;110: 10165–9.
[26] Welch K. Electrodynamic and mechanical spectroscopy method development and analysis relating to materials with biotechnological applications. Acta Universitatis Upsaliensis. Digital Comprehensive Summaries of Uppsala Dissertations from the Faculty of Science and Technology, Uppsala University; 2006. ISBN 91-554-6591-9.
[27] Coelho R. Rev Phys Appl 1983;18:137–46.
[28] Schütt HJ, Gerdes E. J Non-Cryst Solids 1992;144:1–13.
[29] Niklasson GA, Jonsson AK, Strømme M. In: Barsoukov Y, MacDonald JR, editors. Impedance spectroscopy. 2nd ed. New York: Wiley; 2005. p. 302.
[30] Almgren M, Edwards K, Karlsson G. Colloids Surf A 2000;174:3–21.
[31] Dubochet J, Adrian M, Chang JJ, Homo JC, Lepault J, McDowall AW, et al. Q Rev Biophys 1988;21:129–228.
[32] Nilsson M, Alderborn G, Strømme M. Chem Phys 2003;295:159–65.
[33] Nilsson M, Strømme M. J Phys Chem B 2005;109:5450–5.
[34] Baranov AI, Anisimova VN, Khripunov AK, Baklagian YG. Ferroelectrics 2003;28:141–51.
[35] Stauffer D, Aharony A. Introduction to percolation theory. 2nd ed. London: Taylor & Francis; 1992.
[36] Zografi G, Kontny MJ. Pharm Res 1986;3:187–94.
[37] Khan F, Pilpel N. Powder Technol 1987;50:237–41.
[38] Bodin A, Ahrenstedt L, Fink H, Brumerb H, Risberg B, Gatenholm P. Biomacromolecules, in press.
[39] Kim D-Y, Nishiyama Y, Kuga S. Cellulose 2002;9:361–7.
[40] Lapid H, Agmon N. J Chem Phys 2005;122:014506.
[41] Kelvin WT. Philos Mag 1871;42:448–52 [published under the name of Sir William Thomson].